LETTER

Anomalous diffusion of DNA on a supported cationic lipid membrane

A Letters Journal Exploring the Frontiers of Physics

February 2015

EPL, **109** (2015) 38002 www.epljournal.org
doi: 10.1209/0295-5075/109/38002

Anomalous diffusion of DNA on a supported cationic lipid membrane

Chen-Ming Chang[1,2(a)], Yuk-Gyn Lau[1(a)], Shu-Ching Ou[1], Tse-Yu Lin[1,2] and Wen-Tau Juan[1,2(b)]

[1] *Institute of Physics, Academia Sinica - Taipei, Taiwan 11529*
[2] *Department of Physics, National Central University - Jhongli, Taiwan 32001*

received 11 November 2014; accepted in final form 21 January 2015
published online 11 February 2015

PACS 82.35.Gh – Polymers on surfaces; adhesion
PACS 87.15.H- – Dynamics of biomolecules
PACS 87.14.gk – DNA

Abstract – We used fluorescence microscopy to investigate the diffusion dynamics of individual DNA molecules on supported cationic lipid membranes. The mean-squared displacement of DNA on the membrane surface showed sub-diffusion associated with a slower DNA conformational relaxation at a short time scale. The evolution of contours of these non-entangled DNA at this short time scale was retained within a "hypothetical tube" of diameter $< 1\,\mu$m. Inhomogeneous DNA-surface interaction along the DNA contour, identified by total internal reflection fluorescence microscopy, suggested a mechanism for the anomalous dynamics of DNA on the membrane.

Dynamics of macromolecules adsorbed on a lipid membrane is a profound subject not only in terms of biological importance but also for its implications in biotechnologies [1–8]. When lipid molecules are in the disordered-fluid phase, the host membrane surface is usually mimicked as a two-dimensional fluid system [6–8]; the dynamics of a polymer adsorbed on a membrane is usually compared with those obtained by theoretical studies of the polymer on a homogeneous rigid substrate [9–11].

Recent research suggests that the adsorbate on the membrane surface introduces rearrangements of the lipids [12–14]. The host membrane is therefore no longer homogeneous. The diffusion dynamics of adsorbed polymers on a membrane surface with inhomogeneities becomes non-trivial. Recently, effects contributed by different types of surface heterogeneities to near-surface polymer diffusion have been intensively investigated by computer simulations [15–21]. One particularly intriguing finding pertains to the reptation-like surface diffusion of polymers in the dilute condition when obstacles or penetrable sticking points exist on the surface [15,16]. On the other hand, the molecular dynamics study of the polymer diffusion on surfaces with the atomic-scale corrugation found no reptation in the simulations [20].

Although many computational studies have predicted that inhomogeneous interactions between polymer and surfaces alter the diffusion dynamics of an adsorbed polymer, to the best of our knowledge, the direct experimental observation evidencing these predictions is still rare. In this study, we use DNA as the model polymer and the supported cationic lipid (CL) membrane as model surfaces to study the surface diffusion of polymers. Through direct visualization of fully spread DNA molecules, we find an anomalous diffusion associated with a slower conformational relaxation of adsorbed DNA at a short time scale. Evolution of the DNA contour and the coexistence of longitudinal and sideways movements of DNA segments within a tube-like region suggest a non-trivial dynamics of these DNA on the membrane at a short time scale. Details of our result will be presented after introducing the experiment.

Our supported CL membranes consist of mixtures of two different lipid molecules, the neutral 1,2-dioleoyl-sn-glycero-3-phosphocholine (DOPC) and the cationic 1,2-dioleoyl-3-trimethylammonium-propane (DOTAP), at two different molar fractions of DOTAP, $\Phi_{DOTAP} = 0.10$ and 0.05, in this experiment. The fully hydrated membrane, with an estimated thickness of 4 to 6 bilayers, is stored in an HEPES buffer solution (10 mM HEPES solution, 30 mM NaCl, 0.5 mM ascorbic acid) for 8 h to equilibrate before the DNA adsorption. The details of membrane

(a) These authors contributed equally to this work.
(b) E-mail: wtjuan@phys.sinica.edu.tw (corresponding author)

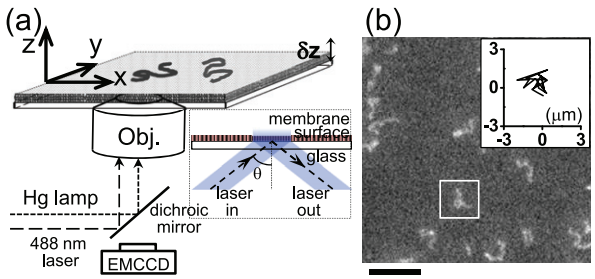

Fig. 1: (Colour on-line) Visualization of diffusion dynamics of DNA molecules on a supported lipid membrane. (a) Schematics of adsorbed DNA molecules, supported cationic lipid membrane, microscope objective (Obj.), and definition of the coordinates. Two different light sources are used for the EFM and TIRFM observations in this experiment. Inset of (a): Decay of the evanescent wave from the substrate with the incident angle $\theta <$ (critical angle) in TIRFM. (b) A typical snapshot of λ-DNA molecules adsorbed on membranes with $\Phi_{DOTAP} = 0.10$ by EFM at t_0. The scale bar is 10 μm. Inset of (b): Center-of-mass trajectory of an adsorbed DNA molecule (outlined in (b)) diffused on the membrane for 20 s starting from t_0.

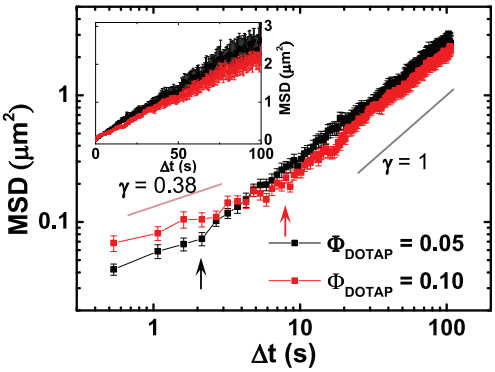

Fig. 2: (Colour on-line) The mean-square displacement (MSD) ($\langle \Delta R^2_{cm}(\Delta t) \rangle$) of DNA molecules diffusing on the membrane with $\Phi_{DOTAP} = 0.10$ and 0.05. Below a critical time scale τ_{MSD} (as indicated by the arrow) for each case of Φ_{DOTAP}, DNA exhibits sub-diffusion. Thin gray and red lines show the reference slopes with $\gamma = 1$ and 0.38, respectively. The inset shows the linear plot of the main graph. Each data point and the associated error bar are calculated by more than 80 independent events.

preparation can be found elsewhere [1]. We then gently introduce YOYO-I labeled λ-DNA (48 kbp), at a stain ratio of 1 dye per 4 bp, into the buffer and allow these DNA to randomly adsorb on the CL membrane surface and gradually spread. Before obtaining the data, we wait for another 2 h, which corresponds to a time scale that is significantly longer than the typical relaxation time of an individual chain upon adsorption [1,11], until the DNA has equilibrated with the membrane surface controlled in the disordered-fluid phase at 25 °C.

Figure 1(a) shows a schematic plot of our experiment. Dye-labeled λ-DNA molecules are adsorbed and spread on our supported CL membrane substrate mounted on an inverted microscope. Segments of the adsorbed DNA are distributed within the focal depth δz ($\sim$1 μm) of our 60× oil immersion objective. We apply two fluorescence microscopy techniques in this experiment: Epifluorescence microscopy (EFM) and total internal reflection fluorescence microscopy (TIRFM), with two different excitation light sources/paths from a mercury lamp and a 488 nm diode-pumped solid-state laser, are employed to observe the dynamics of adsorbed DNA and to identify the polymer-surface distance, respectively. The fluorescent images of the dye-labeled DNA are recorded by a cooled EMCCD camera (Andor DU887).

Figure 1(b) shows a typical snapshot of DNA molecules adsorbed on membranes with $\Phi_{DOTAP} = 0.10$ at a time t_0 by EFM. Since the entire adsorbed DNA, uniformly labeled with YOYO-I dye, on the membrane surface lies in the depth of our focal plane (the upper surface of the glass substrate), the fluorescence intensity of each pixel of the image fairly reflects the local monomer density within the imaging area of a pixel (1 pixel = 0.264 μm × 0.264 μm).

The center-of-mass (CM) position of a DNA molecule at a given time t, $\mathbf{R}_{cm}(t)$, is calculated by $\mathbf{R}_{cm}(t) = \int \mathbf{r} I(\mathbf{r},t) \mathrm{d}\mathbf{r} / \int I \mathrm{d}\mathbf{r}$, where $I(\mathbf{r},t)$ stands for the measured fluorescent intensity at location $\mathbf{r}(t)$. Therefore, the trajectory of the adsorbed DNA starting from an arbitrary initial time t_0 for a time period Δt is obtained. Inset of fig. 1(b) shows the trajectory of the molecule outlined in fig. 1(b) with $\Delta t = 20$ s. The diffusion dynamics of the DNA on the membrane can be characterized by analyzing the trajectories of the adsorbates.

The mean-square displacement (MSD), $\langle \Delta R^2(\Delta t) \rangle \equiv \langle [R(t_0 + \Delta t) - R(t_0)]^2 \rangle$, is a well-known indicator to describe the diffusion dynamics of a mobile object with its position evolution described by $\mathbf{R}(t)$. The power-law dependence of MSD on a different time scale Δt, which can be generalized to $\langle \Delta R^2(\Delta t) \rangle \sim \Delta t^{\gamma}$, is used to categorize the diffusion into different types. The anomalous diffusion in cases with $\gamma \neq 1$ is always interesting [22,23]. It implies that the non-Brownian diffuser is establishing a time correlation of its motion in a Δt regime if $\gamma \neq 1$ is found in the same time regime. The cases with $\gamma < 1$ (>1) are usually referring to sub- (super-) diffusion, respectively.

Figure 2 shows the evolution of MSD ($\langle \Delta R^2_{cm}(\Delta t) \rangle$) *vs.* Δt of DNA adsorbed on membranes with different Φ_{DOTAP}. In the linear plot shown in the inset of fig. 2, the MSD of DNA on the membrane with $\Phi_{DOTAP} = 0.05$ is higher than that in the case of $\Phi_{DOTAP} = 0.10$ over a wide Δt range. This suggests that overall DNA diffusion is faster on a membrane surface having lower charges. Detailed comparisons between cases of two tested Φ_{DOTAP} are shown on the logarithmic MSD in the main panel of fig. 2. The Δt dependence of γ can be derived from the evolution of the apparent slope of the MSD curve in a logarithmic plot. A straight gray line with $\gamma = 1$ is plotted as

the reference for normal diffusion. It is found that diffusions of adsorbed DNA on membranes with two different charge densities both exhibit normal diffusion at long time scales (large Δt). However, trends of their normal diffusions do not extend to short time scale limits. Both MSD curves show $\gamma < 1$ (≈ 0.38) in the small Δt regime. There exists characteristic time scales $\tau_{MSD}(\Phi_{DOTAP})$, where $\tau_{MSD}(0.10) \approx 8\,\mathrm{s}$ and $\tau_{MSD}(0.05) \approx 2\,\mathrm{s}$, indicating the transition time scale of sub- to normal diffusion. The $\tau_{MSD}(0.10) > \tau_{MSD}(0.05)$ suggests a quicker onset of normal diffusion on the membrane with lower charges ($\Phi_{DOTAP} = 0.05$). For a DNA chain under random thermal fluctuations, not only the center-of-mass diffusions, but also the continuous conformational variations of a flexible DNA, are accumulated by the movements of the segments in a molecular chain.

To characterize the conformational change of DNA, we establish a measurement to describe the relaxation of an adsorbed DNA contour over time by an image-matching method. Our algorithm is similar to an IDL code[1]. The conformation-correlation $CC(\Delta t)$, which is the autocorrelation of two 32×32 pixels images centered at the DNA CM between t_0 and $t_0 + \Delta t$, is calculated as $CC(\Delta t) = \frac{\sum[I(\mathbf{r}-\mathbf{R}_{cm},t_0+\Delta t)\times I(\mathbf{r}-\mathbf{R}_{cm},t_0)]}{[\sqrt{\sum I^2(\mathbf{r}-\mathbf{R}_{cm},t_0+\Delta t)}\sqrt{\sum I^2(\mathbf{r}-\mathbf{R}_{cm},t_0)}]}$. We further consider the factor contributed by the decay of the fluorescent signal due to photobleaching. Therefore, we calculate the normalized $CC(\Delta t)$ by $CC_{norm}(\Delta t) \equiv [CC(\Delta t) - CC_{min}]/[CC(0) - CC_{min}]$, where CC_{min}, the anticipated minimum value of the autocorrelation, is obtained by the ensemble-averaged correlation of two distinct DNA molecules at a random pickup time.

Figure 3 shows the $CC_{norm}(\Delta t)$ *vs.* Δt of the ensemble of DNA on membranes with $\Phi_{DOTAP} = 0.10$ and 0.05. In the log-linear plot of $CC_{norm}(\Delta t)$, we found that the decay of the measured $CC_{norm}(\Delta t)$ shows two distinctive trends at short and long time scales. We have fitted these trends with visual reference guidelines to illustrate the characteristics of these trends within different time scales. It also helps us to identify the characteristic time scale of the change in trends. For the case with $\Phi_{DOTAP} = 0.10$, $CC_{norm}(\Delta t)$ decays slower when $\Delta t < 8\,\mathrm{s}$, in comparison to its long time trends (a relatively steeper slope when $\Delta t > 8\,\mathrm{s}$). A similar transition for two-stage decay is also observed for the membrane with $\Phi_{DOTAP} = 0.05$. This suggests that the relaxation of the DNA contour on the membrane surface is, in general, slower at the short time scale.

The characteristic time scale $\tau_{CC}(\Phi_{DOTAP})$, indicating the crossover time scale of two distinctive trends for each case, is particularly interesting. A comparison of the characteristic time scales $\tau_{MSD}(\Phi_{DOTAP})$ and $\tau_{CC}(\Phi_{DOTAP})$ in terms of the MSD (fig. 2) and CC_{norm} (fig. 3) reveals that they share almost identical time scales for the membrane with the same charge density, although the MSD is related to the CM diffusion of DNA and the CC_{norm} is related to the intramolecular-level DNA contour relaxation due to the segment rearrangement, relative to its CM. Our analysis suggests that anomalous DNA diffusion seems to be relevant to the conformation relaxation. Resolving the detailed dynamics of the DNA contour on the membrane surface may shed light on this interesting coincidence at characteristic time scales.

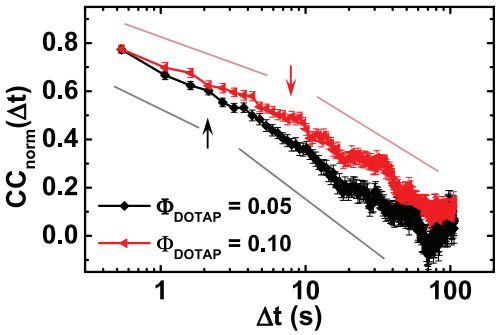

Fig. 3: (Colour on-line) Ensemble-averaged conformational relaxation of adsorbed DNA molecules on membranes with different Φ_{DOTAP}. The linear-log plot is of the conformation-correlation function $CC_{norm}(\Delta t)$. With the straight lines as visual references, the conformation relaxation of DNA on the membranes with $\Phi_{DOTAP} = 0.10$ and 0.05 both show two distinct trends separated by a characteristic $\tau_{CC}(\Phi_{DOTAP})$ (as indicated by arrows) at both short and long time scales.

We therefore try to identify the spatiotemporal evolution of the contour of a DNA chain. We use the simplified contour line to describe the shape of the DNA conformation. The contour line of a DNA is obtained by connecting the central points of two edges of a DNA contour (see inset of fig. 4). Figure 4 shows the evolution of a DNA molecule on the membrane surface with $\Phi_{DOTAP} = 0.10$ through overlaid DNA contour lines over a time interval 18.36 s. At first glance, the contour lines of the adsorbed DNA molecule seem to be retained within a "hypothetical tube" of diameter $< 1\,\mu\mathrm{m}$ in the short time scale ($\Delta t = 0$–$4.86\,\mathrm{s}$). When time evolves, the chain starts de-caging from the "tube" at about $\Delta t = 7.56\,\mathrm{s}$ ($\approx \tau_{CC}(0.10)$) and then loses the memory of its initial conformation at t_0. The finite lifetime of the DNA contour, or the "hypothetical tube", reminds us of classical reptation model: Polymer segments are confined by the surrounding molecules and tend to move along an imaginary tube in a highly concentrated polymer solution [24,25]. However, the observed dynamics in fig. 4 is different from the classical reptation model in two different aspects. First, the de-caging of DNA from the "hypothetical tube" is not initiated from either one of the free ends but is more likely from the middle of the "tube". Second, the wiggly sideways movement in the figure indicates less relevance to the worm-like dynamics.

We are curious about the dynamics of the DNA segment within the time scale during which the chain conformation is retained. The fluorescence intensity of a DNA image in a localized region barely reflects the corresponding

[1]Section "Image Manipulation" on `http://idlastro.gsfc.nasa.gov/contents.html`.

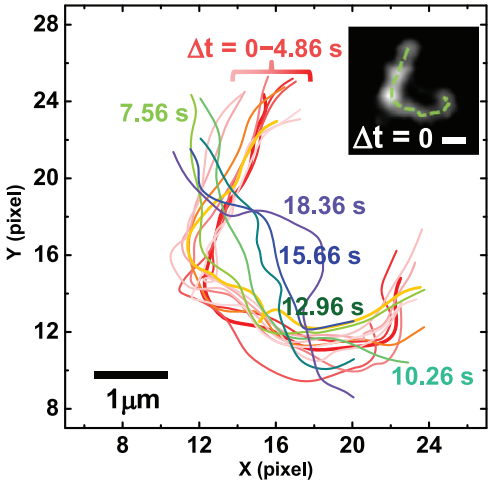

Fig. 4: (Colour on-line) Spatiotemporal evolution of the contour line of an adsorbed DNA molecule on a membrane. The overlaid DNA contour lines over the time interval 18.36 s of the molecule (outlined in fig. 1(b)) show the evolution of its contour on the membrane surface with $\Phi_{DOTAP} = 0.10$. Inset: the dashed line connecting the central points of two edges of a DNA contour between two open ends displays the contour line of the molecule at t_0 ($\Delta t = 0$). The scale bar is 1 μm.

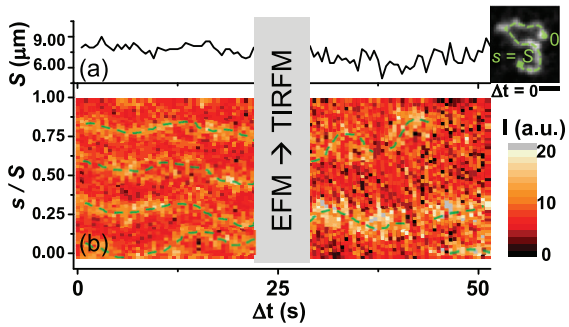

Fig. 5: (Colour on-line) Evolution of the fluorescence intensity of a DNA molecule adsorbed on a membrane surface along its contour line. The image on the upper-right corner shows the snapshot of this demo DNA at t_0, the corresponding contour line, and the positions of $s = 0$ and S. The scale bar is 1 μm. (a) Evolution of the accumulated length of contour line S starting from t_0 ($\Delta t = 0$) with the DNA conformation shown by the image. (b) Evolutions of fluorescence intensity $I(s, \Delta t)$ along the contour line observed by EFM ($\Delta t < 23$ s) and TIRFM ($\Delta t > 29$ s). The hand-drawn dashed green lines indicate the location of the bright bands. $\Phi_{DOTAP} = 0.10$ in this case.

regional population of the DNA segment in this experiment. Tracing the fluorescent signal along the contour line of a DNA image reveals the spatial variation of segment density within the DNA contour. We first parameterize the contour line of a DNA image as s. The two open ends of the contour line correspond to $s = 0$ and S, where S is the accumulated length of the contour line of a particular snapshot. Figure 5(a) shows the evolution of S from an adsorbed DNA molecule starting at t_0. The fluctuating S over the observation period illustrates the continuous deformation of the DNA contour on the membrane surface under thermal fluctuations.

We further analyze the evolution of the local fluorescence intensity along the contour line $I(s, \Delta t)$ and plot the evolution of $I(s, \Delta t)$ in fig. 5(b). At a fixed Δt, the non-uniform $I(s)$ along s suggests a non-uniform segment density distribution over the contour, which may not be a surprise. However, we observe that features of the inhomogeneous $I(s, \Delta t)$ along s remain for a considerable time scale. The brighter bands indicated by the green dashed lines in fig. 5(b) are good examples. This observation implies that the non-uniform segment density distribution along the contour is not easily randomized by the thermal motion of polymer segments. The gentle evolution of the relative distance between adjacent bands, which corresponds to a considerable amount of DNA segments moving along the contour, indicates that the redistribution of a segment along a contour line within the time scale of a few seconds. This observation suggests the existence of the small-scale longitudinal movement of polymer segments in the "hypothetical tube". The local stretching due to the sideways movement of the contour may be another reason, that contributes the small variation of the inter-band distance.

At the end of the EFM observation in fig. 5(b) at $\Delta t = 23$ s, the excitation light source is switched to the laser for the TIRFM observation (data in $\Delta t > 29$ s). The exponential decay of the evanescent wave away from the interface in TIRFM offers a better resolution for resolving the DNA-surface distance, and in turn, their mutual interaction. By TIRFM, the $I(s, \Delta t > 29\,\text{s})$ is not homogeneous either. Compared to the final $I(s, \Delta t = 23\,\text{s})$ by EFM, a significantly different distribution of $I(s, \Delta t = 29\,\text{s})$ along the contour line is observed at the first TIRFM image. The inhomogeneous $I(s, \Delta t)$ observed by TIRFM ($\Delta t > 29$ s) implies a non-uniform DNA-surface attraction along s. The gradual variation of $I(s)$ over Δt by TIRFM also suggests a non-trivial DNA-surface coupling over time.

As suggested by the non-uniform $I(s)$ of the TIRFM data in fig. 5(b), the inhomogeneity of DNA-surface attraction, distributed on a length scale shorter than the DNA contour size, contributes numerous "sticky points" for a near-surface DNA chain at positions with brighter $I(s, \Delta t > 29\,\text{s})$. Without a significant perturbation, only small-scale thermal motions of weakly adsorbed polymer segments (regions with lower $I(s)$) are allowed under the constraint of these strong sticky points. The conformation of the DNA contour is therefore retained in a tube-like region for a short period of time. One may anticipate that the membrane with lower charges is less sticky to the DNA, and hence the smaller values of τ_{MSD} and τ_{CC} in the case with $\Phi_{DOTAP} = 0.05$.

We now understand that the impression of a "hypothetical tube" in fig. 4 comes from the conformation memory of a DNA chain trapped by "sticking points" on the membrane temporarily. The contour of this "tube" simply

reflects the territory of the DNA diffusion within a short time scale. Although there seems no physical confinement from this purely virtual tube-wall, the weakly adsorbed segments between two strong sticky points on the polymer chain may still slosh along the contour and exhibit the longitudinal movement within the "hypothetical tube". Such a behavior could be described as a non-classical reptation-like dynamics in a very localized section of the entire DNA chain.

It may not be a surprise that the non-uniform interaction between a surface and a chain-like molecule readily alters the near-surface polymer dynamics. The ratcheting granular polymer under a spatial gradient of excitation [26], the reptation dynamics of polymers on a surface with sticky points or obstacles [15,16], and the different scaling of polymer diffusion coefficients on attractive surfaces with variable atomic-scale corrugations [20] are good examples. In this experiment, the non-uniform DNA-membrane interaction should exhibit more active involvement than mere intermolecular entanglement of DNA. This provides a mechanism for anomalous DNA diffusion, the memory of the DNA contour, and the coexistence of longitudinal and sideways movements of DNA segments within a "hypothetical tube" on the membrane surface in the short time scale. While scenarios of polymer surface diffusion have been widely discussed, the displacement of DNA segments along the contour line in fig. 5(b) seems to resemble the non-classical "sticky reptation" scenario proposed in ref. [27]. However, we also want to point out that the near-surface polymer diffusion may be similar to the reptation-like dynamics, but for contingent reasons [20]. Resolving the diffusion of individual polymer chains under the non-uniform polymer-surface attraction provides more detailed insight into this issue. Although we do not yet comprehensively understand the origin of the "sticky points", we speculate that the responsiveness of the lipids in our multi-bilayer membrane system may partially contribute to this effect[2].

* * *

The authors gratefully acknowledge the recipe and suggestions provided by Rädler group, the fruitful interactions with Steven Chu in establishing the foundations of our single-molecule imaging, and the discussions with Kwan-Tai Leung, C. Y. David Lu, Pik-Yin Lai, and C. K. Chan. This work was supported by Ministry of Science and Technology of Taiwan, and by the Academia Sinica Research Program on Nanoscience and Nanotechnology.

[2]We have checked the nature of the inhomogeneous DNA-surface interaction by observing the near-surface dynamics of point-like probe molecules, the dye-labelled plasmid DNA. Our preliminary data indicates that these "sticky points" are not stationary. Their spatial distribution and affinities to plasmids change over time.

REFERENCES

[1] Chang C.-M., Lau Y.-G., Tsai J.-C. and Juan W.-T., *EPL*, **99** (2012) 48008.
[2] Herold C., Schwille P. and Petrov E. P., *Phys. Rev. Lett.*, **104** (2010) 148102.
[3] Bae S. C. and Granick S., *Annu. Rev. Phys. Chem.*, **58** (2007) 353.
[4] Tzlil S. and Ben-Shaul A., *Biophys. J.*, **89** (2005) 2972.
[5] Xie A. F. and Granick S., *Nat. Mater.*, **1** (2002) 129.
[6] Sackmann E., *Science*, **271** (1996) 43.
[7] Maier B. and Rädler J. O., *Phys. Rev. Lett.*, **82** (1999) 1911.
[8] Maier B. and Rädler J. O., *Macromolecules*, **33** (2000) 7185.
[9] Doi M. and Edwards S. F., *The Theory of Polymer Dynamics* (Oxford University Press) 1996.
[10] Källrot N., Dahlqvist M. and Linse P., *Macromolecules*, **42** (2009) 3641.
[11] Yang Q.-H., Qian C.-J., Li H. and Luo M.-B., *Phys. Chem. Chem. Phys.*, **16** (2014) 23292.
[12] Wang B., Zhang L., Bae S. C. and Granick S., *Proc. Natl. Acad. Sci. U.S.A.*, **105** (2008) 18171.
[13] Zhang L. and Granick S., *Proc. Natl. Acad. Sci. U.S.A.*, **102** (2005) 9118.
[14] Hochrein M. B., Leierseder J. A., Golubović J. and Rädler J. O., *Phys. Rev. E*, **75** (2007) 021901.
[15] Desai T. G., Keblinski P., Kumar S. K. and Granick S., *J. Chem. Phys.*, **124** (2006) 084904.
[16] Qian H.-J., Chen L.-J., Lu Z.-Y. and Li Z.-S., *Phys. Rev. Lett.*, **99** (2007) 068301.
[17] Mukherji D. and Müser M., *Phys. Rev. E*, **74** (2006) 010601.
[18] Desai T. G., Keblinski P., Kumar S. K. and Granick S., *Phys. Rev. Lett.*, **98** (2007) 218301.
[19] Desai T. G., Keblinski P. and Kumar S. K., *J. Chem. Phys.*, **128** (2008) 044903.
[20] Mukherji D., Bartels G. and Müser M. H., *Phys. Rev. Lett.*, **100** (2008) 068301.
[21] Hoda N. and Kumar S. K., *Phys. Rev. E*, **79** (2009) 020801.
[22] Juan W.-T. and I L., *Phys. Rev. Lett.*, **80** (1998) 3073.
[23] Juan W.-T., Chen M.-H. and I L., *Phys. Rev. E*, **64** (2001) 016402.
[24] McLeish T. C. B., *Adv. Phys.*, **51** (2002) 1379.
[25] Perkins T. T., Smith D. E. and Chu S., *Science*, **264** (1994) 819.
[26] Lin W.-T., Sun Y.-C., Chang C.-C., Lin Y.-C., Peng C.-W., Juan W.-T. and Tsai J.-C., *Phys. Rev. Lett.*, **112** (2014) 058001.
[27] Sukhishvili S. A., Chen Y., Müller J. D., Gratton E., Schweizer K. S. and Granick S., *Macromolecules*, **35** (2002) 1776.